TWO- VERSUS THREE-DIMENSIONAL LES OF PREMIXED TURBULENT PROPAGATING FLAMES

Salah S. Ibrahim, Ahmed M.S. Ali
Department of Aeronautical and Automotive Engineering,
Loughborough University
Loughborough, Leicestershire, LE11 3TU, UK
s.s.ibrahim@lboro.ac.uk, a.m.ali@lboro.ac.uk

Assaad R. Masri
School of Aerospace, Mechanical and Mechatronic Engineering,
The University of Sydney
Sydney, NSW 2006, Australia
masri@aeromech.usyd.edu.au

ABSTRACT

One of the major controversies about the use of Large Eddy Simulation (LES) in turbulent flows concerns the validity of two dimensional (2D) calculations as opposed to the more time consuming but more relevant three-dimensional (3D) runs. It is conceivable that, for a certain class of problems, two-dimensional LES is adequate and this may well be the case for axisymmetric flows which may even involve recirculation. However, generalisation here is extremely dangerous since practical flow configurations lack symmetry and include complex boundary conditions. Understanding the issues that necessitate the use of 2D versus 3D LES is seen to be important given the huge savings that would be achieved if 2D LES is deemed to be adequate. The objective of this paper is to make comparisons between 2D and 3D LES in a fairly complex flow geometry with a view towards understanding the differences between such computations.

INTRODUCTION

Numerical tools for calculating transient turbulent premixed flames are commonly used by design engineers in a wide range of practical applications such as spark ignition engines, gas turbines and industrial burners. The Large Eddy Simulation (LES) approach is gradually gaining acceptance as a viable tool for simulating turbulent premixed flames (Knikker et al., 2002, Mathew, 2002, Pitsch and De Lageneste, 2002) and is particularly suited for computing flows which involve acoustic instabilities (Varoquie et al., 2002), vortex shedding and flow recirculation. However, processes, which occur at the sub-grid scale (SGS), such as diffusion and combustion, require modelling. Menon and co-workers (2002) have demonstrated the usefulness of LES in computing the complex structure of flames in gas turbine combustors. Numerical simulations of complex reacting flows using 3D-LES is, however, computationally much more expensive than 2D-LES as well as Reynolds Averaged Navier-Stokes (RANS) methods. It may be shown, however, that 2D-LES can be relevant for some flow configurations but a generalisation here cannot be made. Comparisons between 2D and 3D LES for non-reacting flows were, for example, reported by Proctor (1998) for wake vortex modelling. They found 2D-LES simulations to be generally valid for wake vortex transport, while 3D-LES gives realistic treatment of the decay for the wake vortices. For reacting flows, Thibaut and Candel (1998) have reported results from 2D-LES calculations of turbulent premixed combustion and concluded that the dynamics of the flame was realistically reproduced. Another example of applying 2D-LES to reacting flows was that reported by Furby and Lofstrom (1994) for their study on bluff body stabilized flames. They stated that realistic trends have been obtained in part of the flow.

This paper reports a comparison between a cost effective 2D-LES simulation, and a more time consuming 3D-LES simulation of turbulent premixed combustion. The flow configuration (shown in Figure (1)) consists of a propagating flame inside a square duct (Cadwallader, 2001) past a turbulence generating grid and a solid obstacle. This combustion chamber provides a well-defined model problem which enables careful assessment of the 2D and 3D simulations. Comparisons are made for the flame structure, speed, and the generated overpressure. Quantitative comparisons between calculated 2D and 3D results of the reaction rate and the eddy viscosity are also presented and discussed.

LES MODEL

Numerical calculations are made using a computational fluid dynamics (CFD) code (Kirkpatrick et al., 2002) for transient compressible turbulent flows. The code uses the large eddy simulation (LES) technique to solve conservation equations for mass, momentum, internal energy and a reaction progress variable (Bray et al., 1985) describing the rate of chemical reaction. The spatial discretisation of the momentum equations within the chamber uses second-order central differences for diffusion, advection and pressure gradient terms. In the

region of the domain outside the chamber where accuracy is less important, the grid is expanded towards the boundaries. Here the third-order accurate QUICK scheme of Leonard (1987) is used to maintain stability. Second-order central differences are also used for the pressure correction equation. The discretisation of the scalar equations uses central differences for the diffusion term and the SHARP scheme (Leonard, 1988) for the advection terms.

The full set of equations is advanced in time using a fractional step method for compressible reacting flows (Kirkpatrick et al., 2003). The Crank-Nicolson scheme is used for the time integration of momentum and scalar equations. The initial conditions are quiescent with zero velocity and reaction progress variable. The fuel mass fraction and properties are set to correspond to those used in the experiment. Ignition is modelled by setting the reaction progress variable to 0.5 in a 5mm radius semi-circle (2D) or hemisphere (3D) centred in the ignition plate at the base of the combustion chamber.

The equations, discretised as described above, are solved using a Bi-Conjugate Gradient solver with an MSI pre-conditioner for the momentum, scalar and pressure correction equations. The time step, δt, is limited to ensure the Courant number remains less than 0.5 with the extra condition that δt=0.3ms. A converged solution was reached when residuals for the momentum and scalar equations were less than 2.5e-5 and 2.0e-3, respectively. The mass conservation error is less than 5.0e-8. A non-uniform grid of 74x327 (in the y-z directions) was used for the 2D calculations on a Dell Precision 530 computer requiring 90MB RAM. The 3D calculations were carried out on a non-uniform grid of 74x74x327 (in the x, y, z directions) using 1.2GB RAM.

Governing equations

Compressible forms of Favre-filtered equations for mass, momentum, and scalars are solved. The general form for the filtered equations is written as follows:

$$\frac{\partial\left(\overline{\rho}\,\tilde{\phi}\right)}{\partial t}+\frac{\partial\left(\overline{\rho}\,\tilde{u}_j\,\tilde{\phi}\right)}{\partial x_j}+\frac{\partial\left(\overline{\rho}\,\widetilde{u_j''\phi''}\right)}{\partial x_j}=S_\phi \qquad (1)$$

For this reacting flow, additional equations for the specific enthalpy, $\tilde{h}$, and the reaction progress variable, $\tilde{c}$ are written:

$$\frac{\partial(\overline{\rho}\tilde{h})}{\partial t}+\frac{\partial(\overline{\rho}\tilde{u}_j\tilde{h})}{\partial x_j}=\frac{\partial\overline{P}}{\partial t}+2\overline{\mu}[\tilde{S}_{ij}-\frac{1}{3}\delta_{ij}\tilde{S}_{kk}]:\frac{\partial\tilde{u}_j}{\partial x_j}, \qquad (2)$$

$$+\frac{\partial}{\partial x_j}(\frac{\overline{\mu}+\overline{\mu}_{SGS}}{\mathrm{Pr}}\frac{\partial\tilde{h}}{\partial x_j})+\overline{\dot{q}_c}$$

$$\frac{\partial(\overline{\rho}\tilde{c})}{\partial t}+\frac{\partial}{\partial x_j}(\overline{\rho}\tilde{u}_j\tilde{c})=\frac{\partial}{\partial x_j}(\frac{\overline{\mu}+\overline{\mu}_{SGS}}{Sc}\frac{\partial\tilde{c}}{\partial x_j})+\overline{\dot{w}_c} \qquad (3)$$

where the last term in Equation (2), $\overline{\dot{q}_c}$ is the chemical source term and the last term in Equation (3), $\dot{w}_c$ is the reaction rate term which was modelled as described later.

In Equations (2) and (3), gradient transport has been used for the SGS turbulent fluxes, where μ_{SGS} is obtained from a SGS eddy viscosity model and *Pr* and *Sc* are the turbulent Prandtl and Schmidt numbers having values of 0.7 and 0.4, respectively.

The SGS eddy viscosity model. The SGS eddy viscosity, μ_{SGS} is calculated here using the dynamic eddy viscosity model due to Germano et al. (1991).and takes the following form:

$$\mu_{SGS}=\overline{\rho}(c_s\overline{\Delta})^2\left|\tilde{S}\right| \qquad (4)$$

where $\overline{\Delta}$ is the filter width expressed as:

$$\overline{\Delta}=2(\Delta x\Delta y\Delta z)^{1/3} \qquad (5)$$

where Δx, Δy and Δz are the local mesh spacing in x, y and z directions, shown in Figure (1).

The model coefficient, c_s, in Equation (4) is calculated dynamically from local instantaneous flow conditions as described by Moin et al. (1991). Therefore, it has the crucial advantage that the viscosity responds properly to local flow structures.

The reaction rate model. The last term in the RHS of Equation (3) represents the filtered chemical reaction rate term $\dot{w}_c$. In this paper, the laminar flamelet approach for lean to stoichiometric fuel/air mixtures is adopted. For high Reynolds and Damkholer numbers, the mean rate of chemical reaction $\dot{w}_c$, may be expressed as (Bray et al. 1985):

$$\overline{\dot{w}_c}=\rho_u u_L\Sigma \qquad (6)$$

where ρ_u is the density of the unburned mixture ahead of the propagating flame and u_L is the laminar burning velocity. The sub-grid scale flame surface density Σ may either be obtained from a simple algebraic expression (e.g. Boger et al., 1998) or obtained by solving a full transport equation for Σ (e.g. Hawkes and Cant, 2001).

Recent DNS (Boger et al., 1998) and LES (Angelberg et al., 1998) data show that the wrinkling of the SGS flame surface is quite low (the sub-grid flame surface is increased by turbulence by less than 40%). This suggests that the SGS model for premixed combustion does not need to be too refined and, hence, a simple algebraic SGS reaction rate formulation similar to that proposed by Boger et al. (1998) for turbulent premixed combustion is used:

$$\Sigma = 4\beta \frac{\bar{c}(1-\bar{c})}{\bar{\Delta}} \qquad (7)$$

where β is a model constant that takes a value of 1.4. In this formulation, the ratio Δ / β may be considered as the SGS flame wrinkling scale. Sensitivity of the model performance to the value of β can be found in Kirkpatrick et al. (2002).

Boundary and initial conditions. Solid boundary conditions are applied at all chamber walls and obstacle solid surfaces with the power-law wall function of Werner and Wengle (1991). A non-reflecting boundary condition is applied at the far field extended outlet (z=1.7m). This is used to prevent reflection of pressure waves at these boundaries.

THE FLOW CONFIGURATION

Figure 1 shows a schematic of the combustion chamber used here. Further details may be found in Cadwallader (2001). A stoichiometric flammable propane mixture in air was settled inside the combustion chamber which was sealed with one layer of household plastic wrap. The chamber consists of a box, 860mm in height, with a square cross section of 150x150mm giving a total volume of 19.6 litres of flammable mixture. The walls are 20mm thick Perspex retained by a steel frame. A glow plug activated by 1.5 volts and placed at the centre of the closed bottom end of the chamber was used to ignite the mixture. A solid square cross section obstruction was placed at 350mm from the closed ignition end imposing an area blockage of 25%. Turbulence inside the chamber was enhanced by placing a grid at 150mm ahead of the ignition source. Flame speed was derived from the highly resolved images of the flame. Further details may be found in Cadwallader (2001).

RESULTS AND DISCUSSION

Figure 2 shows a comparison between calculated and high-speed images of flame shape at selected times after ignition. The reaction progress variable c, is used to show the calculated flame shape. While both 2D and 3D simulations give qualitatively realistic results compared to experiments, the 2D simulations produce a faster flame at all stages of flame propagation. After crossing the turbulence generating grid, the flame becomes highly distorted and this is further exacerbated after crossing the the solid obstruction. The 2D results are leading those from experiments and 3D calculations by about 7ms as seen from the flame images (Figure (2)) as well as from Figure (3) which shows profiles of the flame speed plotted versus time after ignition. Figure (3) shows that at 20ms after ignition, the 2D simulation produces a flame speed of about 40m/s while both 3D simulation and measurements show lower flame speed of about 8m/s. The discrepancy is greatest when the flame starts to interact with the solid obstruction at about 300mm downstream from the ignition end.

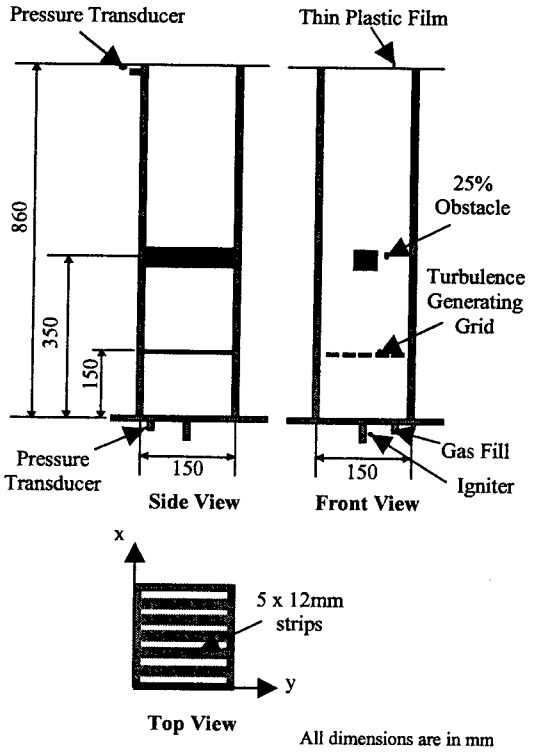

Figure 1: Schematic drawing of the experimental combustion chamber.

Figure (4) shows measured pressure-time traces as well those predicted using 2D- and 3D-LES. It is interesting to note that the peak pressure is similar in both 2D and 3D simulations and is close to the measurement. However, this peak is reached in the 2D-LES about 10ms earlier than both the 3D-LES and the measurements. Another observation worth noting is that in both 2D and 3D simulations, the peak pressure occurs when the flame is interacting with the highly recirculating flow formed behind the solid obstruction. This is also consistent with the measurements. A closer inspection of Figures (3) and (4) show the deviations between the 2D and 3D calculations starts in the quasi-laminar region before the flame reaches the turbulence generating grid.

Snapshots of the eddy viscosity from 2D and 3D simulations are shown in Figure (5) together with the corresponding filtered reaction rate. The comparison is shown when the flame/flow interaction is intense and behind the solid obstruction, i.e. 26ms and 33ms for 2D and 3D calculations, respectively. Although the peak values for the computed reaction rates and eddy viscosity are very much the same for both 2D and 3D, there are subtle differences which can be seen in Figure (5). In 3D, the reaction zone appears to be more turbulent, less structured and closer to the wall than in 2D. Also, The eddy viscosity is more thoroughly spread in 3D and covers the entire width of the chamber with more frequent regions of high viscosity than in 2D runs.

The faster flame propagation resulting from the 2D simulation may be attributed three factors:

- An artificially higher flame surface density in the 2D case resulting from the longer burnt contour per unit area of flow.
- An over-prediction in the turbulent diffusion ahead of the flame. This may be because the 2D-LES does not account properly for the energy dissipation associated with vortex stretching which is a 3D process. This leads to lower dissipation rates and an over-prediction in the energy associated with the large scale flow in the 2D simulation.
- The significance of cross flow effects which are totally ignored in 2D-LES. Cross flow causes a slower flame propagation from the centre of the combustion chamber towards the side walls parallel to the main direction of flame propagation. This can be seen from the 3D results presented in Figures (2) and (3). In the 3D simulations, cross flow effects found to cause an overall reduction in the flame acceleration along the chamber axis.

CONCLUSIONS

Two- and three-dimensional Large Eddy Simulations have been carried out for turbulent propagation flame inside a premixed combustion chamber with built-in turbulence generating grid and a square solid obstruction. Overall, good level of agreement has been obtained between the 3D-LES results and the measurements.

It is found that 2D-LES leads to artificially faster flame propagation rates but realistic peak levels of overpressure. The discrepancies in the 2D-LES may result from cross-flow effects, larger flame surface density and lower dissipation rates.

Acknowledgment. The third author acknowledges the financial support received from the Leverhulme Trust, UK. Professor Masri is also supported by the Australian Research Council.

REFERENCES

Angelberg, C., Veynante, D., Egolfopoulos, F. and Poinsot, T., 1998, "Large eddy simulations of combustion instabilities in premixed flames", *Proceedings, The Centre of Turbulent Research*, Stanford University.

Boger, M., Veynante, D., Doughanem, H. and Trouvee, M., 1998, "Direct numerical simulation analysis of flame surface density concept for large eddy simulation of turbulent premixed combustion", *Proc. Combust. Inst.*, Vol. 27, p. 917.

Bray, K.N.C., Libby, P.A. and Moss, J.B., 1985, *Combust. Flame*, vol. 61, pp. 87-102.

Cadwallader, B.J., 2001, "Experimental Investigation of Premixed Flame Propagation Past an Obstacle", B.Sc. thesis, the University of Sydney.

Furby, C. and Lofstrom, C., 1994, "Large eddy simulations of bluff body stabilized flames", *Proc. Combust. Inst.*, Vol. 25, pp. 1257-1264.

Germano, M., Piomelli, U., Moin, P. and Cabot, W.H., 1991, "A dynamic subgrid-scale eddy viscosity model", *Phys Fluids*, A 3, pp. 1760-1765.

Hawkes, E.R. and Cant, R.S., 2001, "Implications of a flame surface density approach to large eddy simulation of a premixed turbulent combustion", *Combust. Flame*, Vol. 126, pp. 1617-1629.

Kirkpatrick, M., Armfield, S.W., Masri, A.R. and Ibrahim, S.S., 2002, "Numerical issues in large eddy simulation of premixed turbulent propagating flames", *Proceedings of The Second Mediterranean Combustion Symposium*, Sharm El-Sheikh, Egypt, pp. 346-371.

Kirkpatrick, M.P., Armfield, S.W., Masri, A.R., and Ibrahim, S.S., 2003, "Large eddy simulation of propagating turbulent premixed flames; numerical issues", *Flow, Turbulence and Combustion* (in press).

Knikker, R., Veynante, D. and Meneveau, C., 2002, "A priori testing of a similarity model for large eddy simulations of turbulent premixed combustion", *Proc. Combust. Inst.*, Vol. 29, (in press).

Leonard, B. P., 1987, "Sharp simulation of discontinuites in highly convective steady flow", NASA Technical Memorandum 100240.

Leonard, B. P., 1988, AIAA/ASME/SIAM/APS First National Fluid Dynamics Congress, pp.226--231.

Mathew, J., 2002, "Large eddy simulation of a premixed flame with approximate deconvolution modelling", *Proc. Combust. Inst.*, Vol. 29, (in press).

Menon, S., 2002, "Swirl control of combustion instabilities in a gas turbine combustor", *Proc. Combust. Inst.*, Vol. 29, (in press).

Moin P., Squires K., Cabot W. and Lee S., 1991, "A dynamic subgrid-scale model for compressible turbulence and scalar transport", *Phys. Fluids*, A, 3, pp. 2746-2757.

Pitsch, H. and De Lageneste, D., 2002, "Large eddy simulation premixed turbulent combustion using a level-set approach", *Proc. Combust. Inst.*, Vol. 29, (in press).

Proctor, F.H., 1998, "The NASA-Langley wake vortex modelling effort in support of an operational aircraft spacing system", *AIAA-98-0589*.

Thibaut, D. and Candel, S., 1998, "Numerical study of unsteady turbulent premixed combustion: application to flashback simulation", *Combust. Flame*, vol. 113, pp. 53-65.

Varoquie, B., Legier, J.P., Veynante, D. and Poinsot, T., 2002, "Experimental analysis and large eddy simulation to determine the response of non-premixed flames submitted to acoustic forcing", *Proc. Combust. Inst.*, Vol. 29, (in press).

Werner, H. and Wengle, H., 1991, "Large eddy simulation of turbulent flows over and around a cube in a plate channel", *Eighth Symposium on Turbulent Shear Flows*, 19-4-1 to 19-4-6.

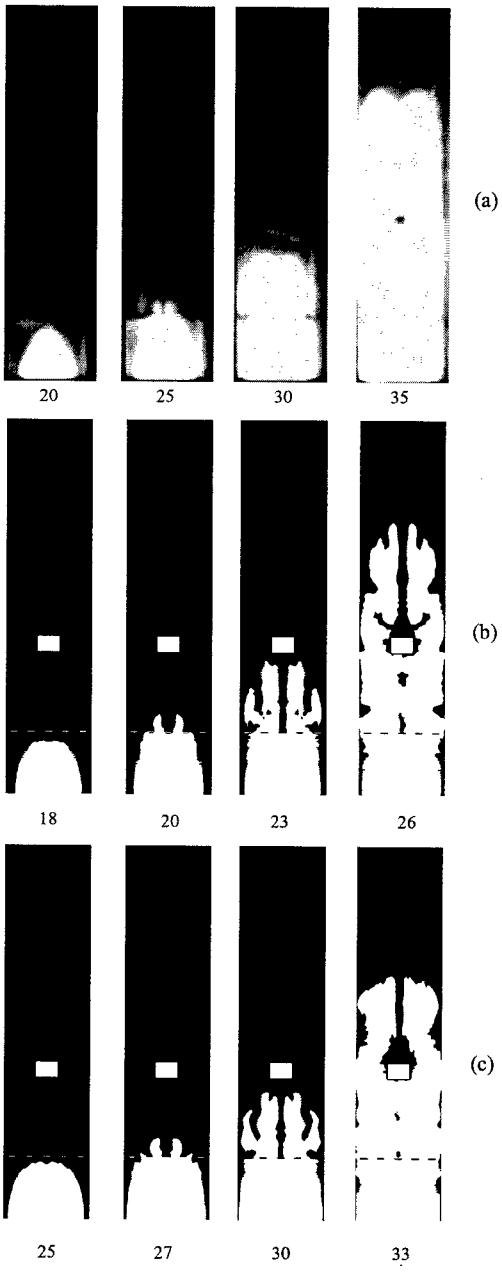

Figure 2: Comparison between (a) measured, (b) 2-D and (c) 3-D flame shape at different times after ignition in milliseconds.

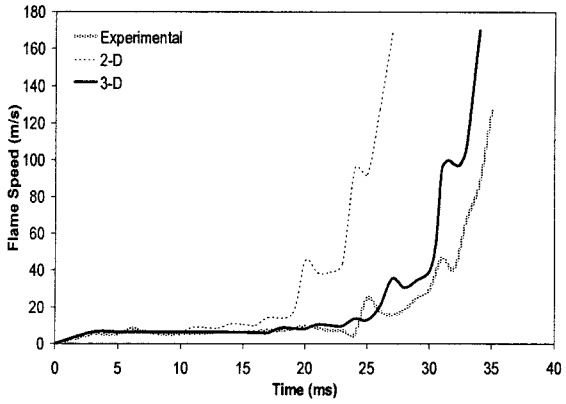

Figure 3: Comparison between measured and calculated flame front speed at different times after ignition.

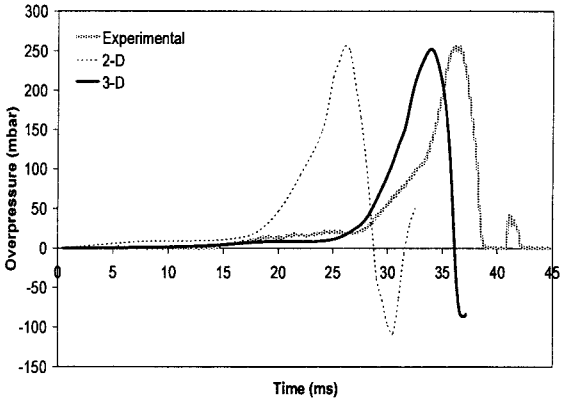

Figure 4: Comparison between calculated and measured pressure time history inside the combustion chamber.

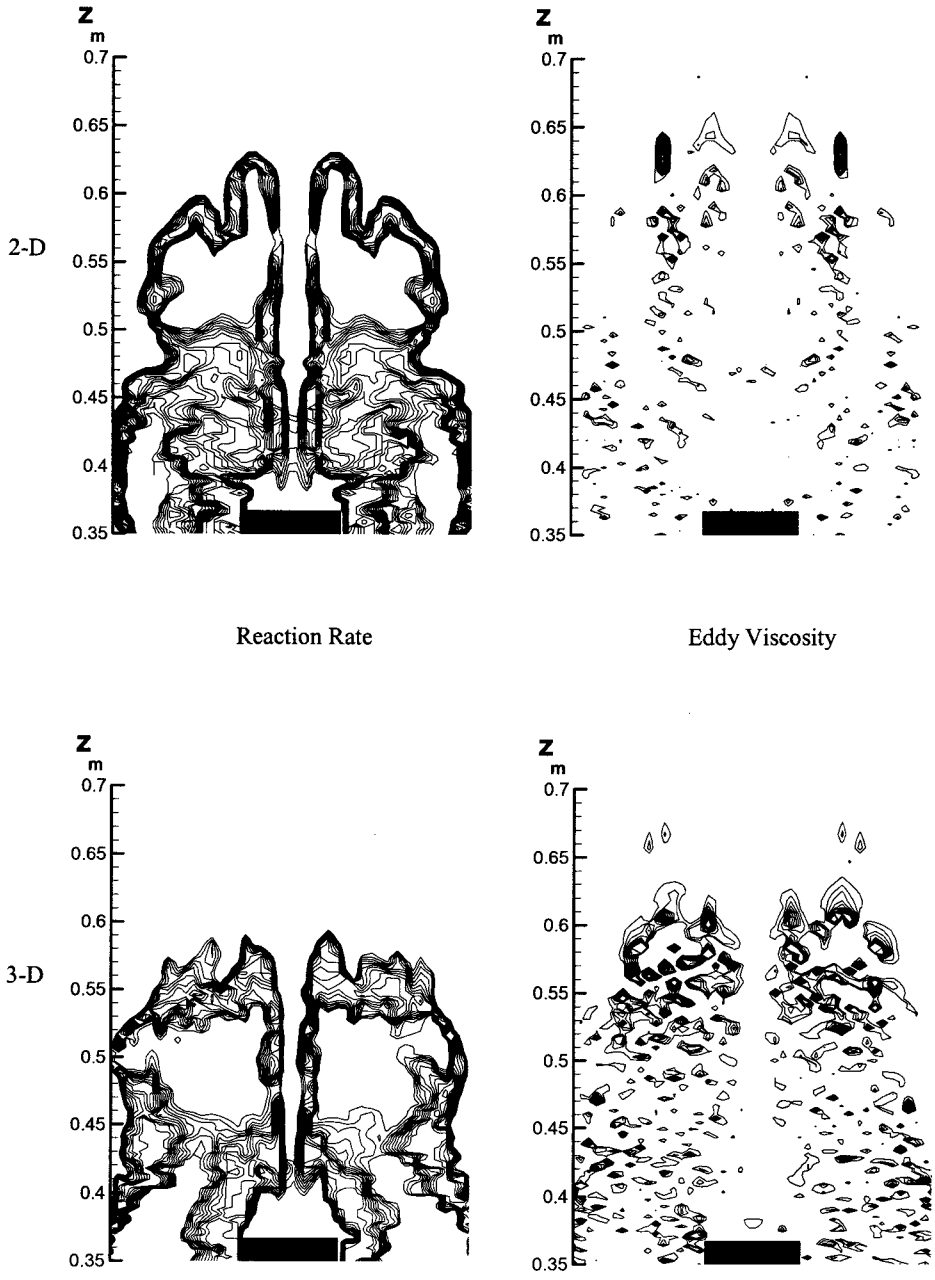

Figure 5: Two- and Three- dimensional calculations of filtered reaction rate and SGS eddy viscosity during flam/flow interactions behind the solid obstacle. Times shown are 26ms for 2-D and 33ms for 3-D. The maximum reaction rate contour is 130 kg/s and the maximum eddy viscosity contour is 2.5×10^{-3} Pa/s for both 2-D and 3-D.